

# VIBRATION OF ELECTRICALLY ACTUATED MEMS TIMOSHENKO MICROBEAMS BASED ON A HIERARCHICAL BEAM ELEMENT

Cong Ich Le<sup>1,\*</sup> , Dinh Kien Nguyen<sup>2,3</sup> 

<sup>1</sup>*Le Quy Don Technical University, 236 Hoang Quoc Viet street, Hanoi, Vietnam*

<sup>2</sup>*Graduate University of Science and Technology, VAST, Hanoi, Vietnam*

<sup>3</sup>*Institute of Mechanics, VAST, Hanoi, Vietnam*

\*E-mail: [lecongich79@lqdtu.edu.vn](mailto:lecongich79@lqdtu.edu.vn)

Received: 30 November 2022 / Published online: 30 December 2022

**Abstract.** In this paper, vibration of Timoshenko microbeams with an axial force in micro-electromechanical systems (MEMS) is studied for the first time by using a nonlinear finite element procedure. Based on the von Kármán geometric nonlinearity and the modified couple stress theory (MCST), a beam element is formulated by employing hierarchical functions to interpolate the displacement field. Using the derived element, the discretized equation of motion for the microbeam is constructed and then solved by the Newton-Raphson iterative procedure in conjunction with the Newmark method. The natural frequencies, pull-in voltages and dynamic deflections are computed for a clamped-clamped microbeam under electrostatic actuation of a given direct current (DC) voltage. The numerical result reveals that the axial force and the microsize effect have a significant influence on the vibration, and the fundamental frequency of the microbeams is underestimated by ignoring the size effect. The effects of the axial force, the applied voltage and the material length scale parameter on the vibration of the beam are studied in detail and highlighted.

*Keywords:* Timoshenko microbeam, MCST, electrostatic actuation, hierarchical interpolation, nonlinear finite element analysis.

## 1. INTRODUCTION

Since the discovery of micro-electromechanical systems (MEMS), their development has reached a level of maturity that, today, several MEMS devices are being used in our every-day life. Microbeams are used in many MEMS devices such as capacitive MEMS switches and resonators, filters, and resonant sensors. This device can be designed by using the electroplating techniques, low temperature processes, and dry releasing techniques [1]. The properties of MEMS such as the frequencies and pull-in voltages can be determined by M-test method [2]. The simulation method, an effective tool in design

and optimization of MEMS, are increasingly used in predicting mechanical characteristics of MEMS elements, e.g. the natural frequencies and pull-in voltages of microbeams in MEMS. Regarding the microbeam in MEMS considered herein, under the electric actuation, the microbeam often undergoes moderately large deflection, and this feature requires nonlinear static and dynamic analyses for accurately assessing mechanical characteristics of the MEMS microbeams. Both analytical and numerical methods have been employed by researchers in predicting the vibration characteristics of microbeams actuated by electric forces in MEMS.

In the early works, the classical beam theories which ignore the influence of the microsize effect have been used in modeling microbeams in MEMS. In [3], Choi and Lovell adopted the classical Euler-Bernoulli beam theory to describe the deformation of the microbeams in MEMS, and then determined the response of the microbeams the shooting method based numerical procedure. The Galerkin method was employed by several authors, for example Abdel-Rahman et al. [4], Younis et al. [5], Younis and Nayfeh [6], in assessing the frequencies and pull-in voltages of microbeams under static and dynamic actuations. The influence of the axial force which resulted from residual stresses in the fabrication process was also considered by Younis and Nayfeh [6]. Abdel-Rahman and Nayfeh [7] investigated the response of a microbeam-based resonant sensor to superharmonic and subharmonic electric actuations by using a nonlinear beam model. The perturbation method was adopted by the authors to derive the first-order nonlinear differential equations for the microbeam, and the Galerkin method was also used to determine the static and dynamic pull-in voltages. The influence of both the axial force and the viscous damping effect on the response of the microbeam was considered in the work. Chatterjee and Pohit [8] presented a large deflection model for investigating the pull-in phenomenon of microcantilever with a relatively large gap between the microbeam and the stationary electrode. The authors concluded that the geometric nonlinearity plays a significant role when pull-in occurs. Various problems on vibration and bending of microbeams in MEMS have been considered in the textbook by Younis [9]. The effects of geometric nonlinearity, viscous damping and axial force on the microbeams behavior have been taken into account. The influence of residual stresses and axial force on pull-in voltages of microbeams was considered by Rezazadel et al. [10]. The governing equation of the microbeam was derived in the basis of Euler-Bernoulli beam theory and solved by the finite difference method. Finite element method was used in [11] to study the pull-in instability phenomenon of microbeams. Euler-Bernoulli beam theory was also adopted in the work to model the microbeam deformation. The COMSOL multi-physics finite element package was employed by Kaneria et al. [12] to study the pull-in instability of microcantilever in MEMS devices. A nonlinear model for studying the nonlinear electrostatic pull-in behavior of shaped actuators in micro-electro-mechanical systems was proposed by Kuang and Chen [13], taking into account the fringing effects of the electrical field. It was concluded by the authors that the pull-in voltages obtained by the differential quadrature method in the work agree well with the measured data.

The influence of microsize effect on mechanical response of structural elements in MEMS has been considered recently. To this end, various higher-order continuum theories [14, 15] have been proposed and used in combination with conventional structural theories in modelling microstructures. Among the higher-order continuum theories, the modified couple stress theory (MCST) used only parameter, namely the material length scale [16], is widely employed in conjunction with a classical beam theory to model microbeams. In this line of works, Farokhi and Ghayesh [17] used the MCST in combination with Euler-Bernoulli beam theory to construct the governing equations in dynamic analysis of a MEMS microcantilever subjected to an electric excitation. The authors found that the classical beam theory, which ignores the size effect, results in a higher deflection and a lower static pull-in voltage. Ghayesh and Farokhi [18] modelled the electrode of MEMS by a microplate in their study on nonlinear behaviour of MEMS resonators due to electric actuation. The geometric nonlinearities, geometric imperfections, small-size effects, and all the transverse and in-plane inertia and displacements have been taken into account in the microplate model. An analytical method based on the MCST was presented by Baghani [19] for studying the size-dependent static pull-in behaviour of microcantilevers in MEMS. The method employed the modified variational iteration procedure in assessing the nonlinear response of the microbeams to electric actuation. Ghayesh et al. [20] studied nonlinear size-dependent resonant behaviour of MEMS resonators subjected to both DC and alternating current (AC) voltages. Euler-Bernoulli beam theory and the MCST were adopted by the authors in the derivation of the nonlinear differential equations, and Galerkin method was used to obtain the frequency-response curves. Hu et al. [21] presented an analytical approach to the static, dynamic, and stability analysis of a microcantilever subjected to electrostatic forces. Based on numerical investigation, they concluded that the instable regions appear not only near the multiples of resonant frequencies but also near some fractions of resonant frequency differences. Osterberg and Senturia [22] presented a set of electrostatically actuated microelectromechanical test for determining the electrostatic pull-in of cantilever and clamped beams. The proposed method agreed with literature values to within 4%. Recently, Le et al. [23] studied the size dependent behavior of a MEMS microbeam under electrostatic actuation using the improved third-order shear deformation theory of Shimpi and Patel [24]. The authors concluded that the dynamic deflections of the beam are overestimated when ignore the microsize effect.

In this paper, vibration of axially loaded microbeams in MEMS with the pull-in instability phenomenon is studied for the first time by using a nonlinear finite element procedure. In order to account for the size effect, the MCST is employed in conjunction with Timoshenko beam theory to model the microbeams. A nonlinear beam element is formulated and used to construct the discretized equation of motion. In order to avoid the shear-locking problem, the hierarchical functions are employed herein to interpolate the displacement field. As above mentioned, under the electric actuation the microbeam

in MEMS undergoes relatively large deflection, and this large deflection should be computed before evaluating frequencies of the microbeam. To account for this nonlinearity, the von Kármán nonlinear strain-displacement relationship is adopted in the derivation of the beam element. The Newton–Raphson iterative procedure is used in combination with the Newmark method to compute the frequencies, dynamic deflections and pull-in voltages of a clamped microbeam under different axial forces and static voltages. It is worthy to note that in addition to the vibration analysis of the axially load Timoshenko microbeam in MEMS presented herein for the first time, the hierarchical nonlinear beam element derived in the present work are the main novelties of this. The influence of the applied voltage, the axial force as well as the material length scale parameter on the frequencies, the pull-in voltages and the dynamic deflections of the microbeam are studied in detail and highlighted. The dependence of the pull-in voltage at which the instability occurs is also examined and discussed.

## 2. MATHEMATICAL MODEL

Fig. 1 shows a sketch of microbeam with length  $L$ , width  $b$ , thickness  $h$  in MEM. The initial air gap between the microbeam and the stationary electrode is  $d$ , and the applied voltage is denoted by  $V$ .

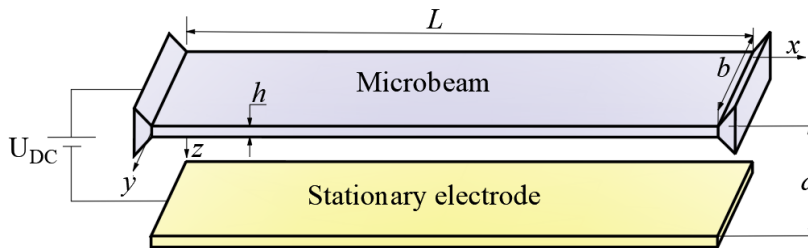


Fig. 1. A sketch of microbeam and stationary electrode in MEMS

The deformation of the microbeam is described herein by using Timoshenko beam theory. According to the theory, the axial displacement ( $u_1$ ) and the transverse displacement ( $u_3$ ) at any point of the beam are given by

$$\begin{aligned} u_1(x, z, t) &= u(x, t) - z\theta(x, t), \\ u_3(x, z, t) &= w(x, t), \end{aligned} \quad (1)$$

where  $z$  is the distance from the midplane to the considering point;  $u(x, t)$  and  $w(x, t)$  are, respectively, the axial and transverse displacements of the corresponding point on the midplane,  $\theta(x, t)$  is the cross-sectional rotation,  $t$  is the time variable.

Based on the von Kármán nonlinearity, the normal strain ( $\epsilon_{xx}$ ) and the shear strains ( $\gamma_{xz}$ ) are given by

$$\begin{aligned} \epsilon_{xx} &= u_{1,x} + \frac{1}{2}u_{3,x}^2 = u_{,x} + \frac{1}{2}w_{,x}^2 - z\theta_{,x}, \\ \gamma_{xz} &= u_{1,z} + u_{3,x} = w_{,x} - \theta, \end{aligned} \tag{2}$$

where a subscript comma is used to indicate the derivative of the variable with respect to the spatial coordinate  $x$ ,  $(\cdot)_{,x} = \partial(\cdot)/\partial x$ .

With the assumption of linear behaviour for the beam material, the stresses are related to the strain according to

$$\begin{Bmatrix} \sigma_{xx} \\ \tau_{xz} \end{Bmatrix} = \begin{bmatrix} E & 0 \\ 0 & \psi G \end{bmatrix} \begin{Bmatrix} \epsilon_{xx} \\ \gamma_{xz} \end{Bmatrix}, \tag{3}$$

where  $\sigma_{xx}$  and  $\tau_{xz}$  are, respectively, the normal and shear stresses,  $G$  is the effective shear modulus; and  $\psi$  is the shear correction factor, taken by  $5/6$  for the beams with rectangular cross section considered herein.

Inasmuch as classical continuum mechanics is not capable of capturing the small-size effects, development of size-dependent elasticity theories is of great importance for analysis of microstructures. The MCST with only one parameter proposed by Yang et al. [16] is employed herewith to derive the the elastic strain energy for the microbeam as

$$U = \frac{1}{2} \int_V (\boldsymbol{\sigma} : \boldsymbol{\epsilon} + \mathbf{m} : \boldsymbol{\chi}) dV, \tag{4}$$

where  $V$  is the volume of the microbeam;  $\boldsymbol{\sigma}$  and  $\boldsymbol{\epsilon}$  are, respectively, the tensors of the stresses and strains;  $\mathbf{m}$  is the deviatoric part of the couple stress tensor and  $\boldsymbol{\chi}$  is the symmetric curvature tensor. With the Timoshenko beam model of the present work, the elastic strain energy in Eq. (4) has the following expression

$$U = \frac{b}{2} \int_0^L \int_{-h/2}^{h/2} (\sigma_{xx}\epsilon_{xx} + \tau_{xz}\gamma_{xz} + 2m_{xy}\chi_{xy}) dz dx, \tag{5}$$

where

$$\chi_{xy} = -\frac{1}{4}(\theta_{,x} + w_{,xx}), \quad m_{xy} = 2Gl^2\chi_{xy}, \tag{6}$$

with  $l$  is the material length scale parameter.

From Eqs. (2), (3) and (6), the strain energy of the beam in Eq. (5) can be recasted in the following form

$$\begin{aligned} U_b &= \int_0^L \left( \frac{EI\theta_{,x}^2}{2} + \frac{EA}{2} \left( u_{,x}^2 + u_{,x}w_{,x}^2 + w_{,x}^4/4 \right) + \frac{GA l^2}{8} (\theta_{,x}^2 + 2\theta_{,x}w_{,xx} + w_{,xx}^2) \right. \\ &\quad \left. + \frac{GA\psi}{2} (\theta^2 - 2\theta w_{,x} + w_{,x}^2) \right) dx, \end{aligned} \tag{7}$$

where  $A = b \times h$  is the cross-sectional area and  $I = bh^3/12$  is the second moment of inertia of the beam cross section.

From Eq. (1) one can write the kinetic energy of the beam in the form

$$T = \frac{\rho}{2} \int_V (\dot{u}_1^2 + \dot{u}_3^2) dV = \frac{\rho A}{2} \int_0^L (\dot{u}^2 + \dot{w}^2) dx + \frac{\rho I}{2} \int_0^L \dot{\theta}^2 dx, \quad (8)$$

with  $\rho$  is the mass density, and the over dot is used to denote the derivative of a quantity with respect to the time variable  $t$ .

The beam is under actuation of the electrostatic force per unit length in the form [10, 18]

$$q(x, t) = \frac{\varepsilon_0 b V_{DC}^2}{2(d - u_3(x, t))^2}. \quad (9)$$

The electrical potential energy  $W_F$  stored between the upper and lower electrodes is given by [21]

$$W_F = - \int_0^L \frac{\varepsilon_0 b V_{DC}^2}{2(d - w)} dx. \quad (10)$$

Furthermore, the microbeam is considered to be axially loaded by a force  $P$ . The energy  $W_P$  caused by the axial force  $P$  is given by

$$W_P = \frac{1}{2} \int_0^L P u_{3,x}^2 dx = \frac{1}{2} \int_0^L P w_{,x}^2 dx. \quad (11)$$

The damping effect is modelled herein by using the Rayleigh dissipation function  $D$ , which has the following form [9]

$$D = \frac{c_0}{2} \int_0^L (\dot{u}^2 + \dot{w}^2) dx, \quad (12)$$

with  $c_0$  is the viscous damping coefficient.

The nonlinear differential equations of motion for the microbeam is derived by using the Hamilton's principle, which can be written as

$$\delta \int_{t_1}^{t_2} (T - (U_b + W_P + W_F + D)) = 0. \quad (13)$$

Eq. (13) leads to a system two nonlinear differential equations of motion. However, a closed-form solution for such nonlinear equations is very difficult to derive. In the present work, finite element method is adopted to derive a discretized equation of motion and to compute the vibration characteristics of the microbeam. To this end, a finite element formulation is derived in the next section.

### 3. FINITE ELEMENT FORMULATION

A finite element formulation is formulated in this Section for constructing the discretized equation of motion and computing nonlinear vibration characteristics of the beam. To this end, the beam is assumed to be divided into a number of two-node beam elements with length  $l_e$ . The displacements  $u_0, w_0$  of a point on the beam mid-axis and the cross-sectional rotation  $\theta$  in Timoshenko beam theory are independent, and linear functions can be adopted to interpolate them from their nodal values. The beam element formulated from the linear interpolation, however encounters the shear-locking problem [25]. To avoid the shear-locking problem, the displacements and rotation are interpolated from their nodal values by using the hierarchical functions as follows [26]

$$u = N_1 u_1 + N_2 u_2, \quad \theta = N_1 \theta_1 + N_2 \theta_2 + N_3 \theta_3, \quad w = N_1 w_1 + N_2 w_2 + N_3 w_3 + N_4 w_4, \quad (14)$$

where  $u_1, u_2, \theta_1, \theta_2, w_1, w_2$  are the degrees of freedom at nodes 1 and 2;  $\theta_3, w_3, w_4$  are the additional degrees of freedom; and  $N_1, N_2, N_3$  and  $N_4$  are the linear, quadratic, and cubic forms of the hierarchical shape functions with the following forms [27]

$$N_1 = \frac{1}{2}(1 - \xi), \quad N_2 = \frac{1}{2}(1 + \xi), \quad N_3 = (1 - \xi^2), \quad N_4 = \xi(1 - \xi^2), \quad (15)$$

with  $\xi = \frac{2x}{l_e} - 1$  being the natural coordinate (with  $l_e$  is the initial element length).

A Timoshenko beam element can be formulated from the interpolation (14) and (15). To make the element more efficient, Tessler and Dong [28] proposed a method by constraining the shear strain to be constant,  $\gamma_{xz} = \text{const}$ . The method allows to express  $w_3$  and  $w_4$  in term of  $\theta_i$  ( $i = 1, \dots, 3$ ), and the interpolation (14), (15) deduces to the following forms [26]

$$\begin{aligned} u &= N_1 u_1 + N_2 u_2 = \mathbf{h}\mathbf{u}, \quad \theta = N_1 \theta_1 + N_2 \theta_2 + N_3 \theta_3 = \mathbf{h}_\theta \boldsymbol{\theta}, \\ w &= N_1 w_1 + N_2 w_2 + \frac{l_e}{8} N_3 (\theta_1 - \theta_2) + \frac{l_e}{6} N_4 \theta_3 = \mathbf{h}\mathbf{w} + \mathbf{h}_w \boldsymbol{\theta}, \end{aligned} \quad (16)$$

where

$$\begin{aligned} \mathbf{u} &= \{ u_1, u_2 \}^T, \\ \boldsymbol{\theta} &= \{ \theta_1, \theta_2, \theta_3 \}^T, \\ \mathbf{w} &= \{ w_1, w_2 \}^T, \\ \mathbf{h} &= \{ N_1, N_2 \}, \\ \mathbf{h}_\theta &= \{ N_1, N_2, N_3 \}, \\ \mathbf{h}_w &= \left\{ \frac{l_e}{8} N_3, -\frac{l_e}{8} N_3, \frac{l_e}{6} N_4 \right\}. \end{aligned} \quad (17)$$

Differentiating in Eq. (16) with respect to  $x$  gives

$$u_{,x} = \mathbf{b}\mathbf{u}, \quad \theta_{,x} = \mathbf{b}_\theta \boldsymbol{\theta}, \quad w_{,x} = \mathbf{b}\mathbf{w} + \mathbf{b}_w \boldsymbol{\theta}, \quad w_{,xx} = \mathbf{c}_w \boldsymbol{\theta}, \quad (18)$$

with

$$\mathbf{b} = \mathbf{h}_{,x}, \quad \mathbf{b}_\theta = \mathbf{h}_{\theta,x}, \quad \mathbf{b}_w = \mathbf{h}_{w,x}, \quad \mathbf{c}_w = \mathbf{b}_{w,x}. \quad (19)$$

Using the above interpolations, one can write the expression of strain energy in Eq. (7) in the following form

$$\begin{aligned} U_b = \sum^{ne_B} U_b^e = \sum^{ne_B} \int_0^{l_e} & \left( \frac{EI(\mathbf{b}_\theta \boldsymbol{\theta})^2}{2} + \frac{EA}{2} \left( (\mathbf{b}\mathbf{u})^2 + (\mathbf{b}\mathbf{u})(\mathbf{b}\mathbf{w} + \mathbf{b}_w \boldsymbol{\theta})^2 + (\mathbf{b}\mathbf{w} + \mathbf{b}_w \boldsymbol{\theta})^4 / 4 \right) \right. \\ & + \frac{GA I^2}{8} \left( (\mathbf{b}_\theta \boldsymbol{\theta})^2 + 2(\mathbf{b}_\theta \boldsymbol{\theta})(\mathbf{c}_w \boldsymbol{\theta}) + (\mathbf{c}_w \boldsymbol{\theta}) \right) \\ & \left. + \frac{GA\psi}{2} \left( (\mathbf{h}_\theta \boldsymbol{\theta})^2 - 2(\mathbf{h}_\theta \boldsymbol{\theta})(\mathbf{b}\mathbf{w} + \mathbf{b}_w \boldsymbol{\theta}) + (\mathbf{b}\mathbf{w} + \mathbf{b}_w \boldsymbol{\theta})^2 \right) \right) dx, \end{aligned} \quad (20)$$

with  $ne_B$  is the total number of elements used to discretize the beam.

The kinetic energy of the beam in Eq. (8) can now be rewritten as

$$T = \sum^{ne_B} T^e = \sum^{ne_B} \left( \frac{\rho A}{2} \int_0^{l_e} \left( (\mathbf{h}\dot{\mathbf{u}})^2 + (\mathbf{h}\dot{\mathbf{w}} + \mathbf{h}_w \dot{\boldsymbol{\theta}})^2 \right) dx + \frac{\rho I}{2} \int_0^{l_e} (\mathbf{h}_\theta \dot{\boldsymbol{\theta}})^2 dx \right). \quad (21)$$

Finally, the work done by the electric force in Eq. (10), the energy  $W_P$  in Eq. (11) and the damping mechanism  $D$  in Eq. (12) are also written in the forms

$$W_F = \sum^{ne_B} W_F^e = \sum^{ne_B} \int_0^{l_e} \frac{-\varepsilon_0 b V_{DC}^2}{2(d - \mathbf{h}\mathbf{w} - \mathbf{h}_w \boldsymbol{\theta})} dx, \quad (22)$$

$$W_P = \sum^{ne_B} W_P^e = \sum^{ne_B} \frac{1}{2} \int_0^L P(\mathbf{b}\mathbf{w} + \mathbf{b}_w \boldsymbol{\theta})^2 dx, \quad (23)$$

$$D = \sum^{ne_B} D^e = \sum^{ne_B} \frac{c_0}{2} \int_0^L \left( (\mathbf{h}\dot{\mathbf{u}})^2 + (\mathbf{h}\dot{\mathbf{w}} + \mathbf{h}_w \dot{\boldsymbol{\theta}})^2 \right) dx. \quad (24)$$

Substituting Eqs. (20)–(24) into Eq. (13), then performing integration over the total beam length results in the following matrix form for the Galerkin residual equation [25] as

$$\sum^{ne_B} (\mathbf{m}_e \ddot{\mathbf{q}}_e + \mathbf{c}_e \dot{\mathbf{q}}_e + \mathbf{k}_e \mathbf{q}_e - \mathbf{f}_e) = 0. \quad (25)$$

In the above equation,  $m_e$ ,  $c_e$  and  $k_e$  denote the mass, damping and stiffness matrices of the element, respectively;  $\dot{\mathbf{q}}_e$  and  $\ddot{\mathbf{q}}_e$  are, respectively, the vectors of the nodal velocities and nodal accelerations of the element;  $\mathbf{f}_e$  is the element vector of the external force.

It is convenient to split the element mass, damping and stiffness matrices into sub-matrices as follows

$$\mathbf{m}_e = \begin{bmatrix} \mathbf{m}_{uu} & \mathbf{m}_{u\theta} & \mathbf{m}_{uw} \\ \mathbf{m}_{u\theta}^T & \mathbf{m}_{\theta\theta} & \mathbf{m}_{\theta w} \\ \mathbf{m}_{uw}^T & \mathbf{m}_{\theta w}^T & \mathbf{m}_{ww} \end{bmatrix}, \quad \mathbf{c}_e = \begin{bmatrix} \mathbf{c}_{uu} & \mathbf{c}_{u\theta} & \mathbf{c}_{uw} \\ \mathbf{c}_{u\theta}^T & \mathbf{c}_{\theta\theta} & \mathbf{c}_{\theta w} \\ \mathbf{c}_{uw}^T & \mathbf{c}_{\theta w}^T & \mathbf{c}_{ww} \end{bmatrix}, \quad (26)$$

$$\mathbf{k}_e = \mathbf{k}_e^b + \mathbf{k}_e^P, \quad \mathbf{k}_e = \begin{bmatrix} \mathbf{k}_{uu} & \mathbf{k}_{u\theta} & \mathbf{k}_{uw} \\ \mathbf{k}_{u\theta}^T & \mathbf{k}_{\theta\theta} & \mathbf{k}_{\theta w} \\ \mathbf{k}_{uw}^T & \mathbf{k}_{\theta w}^T & \mathbf{k}_{ww} \end{bmatrix}, \quad \mathbf{k}_e^P = \begin{bmatrix} \mathbf{0} & \mathbf{0} & \mathbf{0} \\ \mathbf{0} & \mathbf{k}_{\theta\theta}^P & \mathbf{k}_{\theta w}^P \\ \mathbf{0} & (\mathbf{k}_{\theta w}^P)^T & \mathbf{k}_{ww}^P \end{bmatrix}.$$

The sub-matrices of in the above equations are calculated by respectively twice differentiating the kinetic, damping and strain energies of the element as follows

$$\begin{aligned} \mathbf{m}_{uu} &= \frac{\partial^2 T^e}{\partial \mathbf{u}^2}, & \mathbf{m}_{\theta\theta} &= \frac{\partial^2 T^e}{\partial \theta^2}, & \mathbf{m}_{ww} &= \frac{\partial^2 T^e}{\partial \mathbf{w}^2}, \\ \mathbf{m}_{u\theta} &= \frac{\partial^2 T^e}{\partial \mathbf{u} \partial \theta}, & \mathbf{m}_{uw} &= \frac{\partial^2 T^e}{\partial \mathbf{u} \partial \mathbf{w}}, & \mathbf{m}_{\theta w} &= \frac{\partial^2 T^e}{\partial \theta \partial \mathbf{w}}, \end{aligned} \quad (27)$$

$$\begin{aligned} \mathbf{c}_{uu} &= \frac{\partial^2 D^e}{\partial \mathbf{u}^2}, & \mathbf{c}_{\theta\theta} &= \frac{\partial^2 D^e}{\partial \theta^2}, & \mathbf{c}_{ww} &= \frac{\partial^2 D^e}{\partial \mathbf{w}^2}, \\ \mathbf{c}_{u\theta} &= \frac{\partial^2 D^e}{\partial \mathbf{u} \partial \theta}, & \mathbf{c}_{uw} &= \frac{\partial^2 D^e}{\partial \mathbf{u} \partial \mathbf{w}}, & \mathbf{c}_{\theta w} &= \frac{\partial^2 D^e}{\partial \theta \partial \mathbf{w}}, \end{aligned} \quad (28)$$

and

$$\begin{aligned} \mathbf{k}_{uu}^b &= \frac{\partial^2 U_b^e}{\partial \mathbf{u}^2}, & \mathbf{k}_{\theta\theta}^b &= \frac{\partial^2 U_b^e}{\partial \theta^2}, & \mathbf{k}_{ww}^b &= \frac{\partial^2 U_b^e}{\partial \mathbf{w}^2}, \\ \mathbf{k}_{u\theta}^b &= \frac{\partial^2 U_b^e}{\partial \mathbf{u} \partial \theta}, & \mathbf{k}_{uw}^b &= \frac{\partial^2 U_b^e}{\partial \mathbf{u} \partial \mathbf{w}}, & \mathbf{k}_{\theta w}^b &= \frac{\partial^2 U_b^e}{\partial \theta \partial \mathbf{w}}, \\ \mathbf{k}_{\theta\theta}^P &= \frac{\partial^2 W_p^e}{\partial \theta^2}, & \mathbf{k}_{\theta w}^P &= \frac{\partial^2 W_p^e}{\partial \theta \partial \mathbf{w}}, & \mathbf{k}_{ww}^P &= \frac{\partial^2 W_p^e}{\partial \mathbf{w}^2}. \end{aligned} \quad (29)$$

Finally, the element force vector resulted from Eq. (22) is

$$\mathbf{f}_e = \left\{ \mathbf{0} \quad \mathbf{0} \quad \mathbf{f}_e^w \right\}^T, \quad \mathbf{f}_e^w = \mathbf{h}^T q(x, t), \quad (30)$$

where the electrostatic force  $q(x, t)$  defined by Eq. (9) is a function of the current transverse displacement  $w(x, t)$ . It is worthy to emphasize that, in addition to the large deflection, the dependence of the force upon the displacement are two sources of nonlinearity of the problem. As can be seen from in Eq. (25) that the highest order of the functions under the integral symbol is six, thus four Gauss points are necessary to use for computing the integrals exactly.

The obtained mass, damping, stiffness matrices and nodal force vector of the element are assembled into the corresponding structural matrices and vector, and then the discretized nonlinear equation of motion for the microbeam can be constructed as follows

$$\mathbf{M}\ddot{\mathbf{D}} + \mathbf{C}\dot{\mathbf{D}} + \mathbf{K}\mathbf{D} - \mathbf{F} = 0. \quad (31)$$

In the above equation  $\mathbf{D}$ ,  $\dot{\mathbf{D}}$  and  $\ddot{\mathbf{D}}$  are, respectively, the structural vectors of the nodal displacements, nodal velocities and nodal accelerations;  $\mathbf{M}$ ,  $\mathbf{C}$ ,  $\mathbf{K}$  denote the structural mass, damping and stiffness matrices, respectively;  $\mathbf{F}$  is the structural vector force vector; In order to solve the nonlinear equation of motion (31), the Newton–Raphson iterative procedure is employed herein in combination with the Newmark method. In the case of static analysis, the acceleration and velocity vectors  $\ddot{\mathbf{D}}$  and  $\dot{\mathbf{D}}$  are set to zeros, and the nodal displacement vector  $\mathbf{D}$  is computed by using the iterative method only.

#### 4. NUMERICAL RESULTS

The numerical results on vibration analysis of the Timoshenko microbeam in MEMS are reported in this section. Otherwise stated, a clamped-clamped microbeam made of silicon with the following properties [9] is employed in all the computations.

$$E = 169 \text{ GPa}, \quad \rho = 2332 \text{ kg/m}^3, \quad \nu = 0.06. \quad (32)$$

For the element model, a mesh of 8 equal elements is used in all the computations reported the below. The following dimensionless parameters are introduced for the fundamental frequency, the material length scale and the maximum deflection, respectively

$$\mu = \omega_1 \sqrt{\frac{\rho AL^4}{EI}}, \quad \eta = \frac{l^2 AG}{EI}, \quad W_{\max} = \max\left(\frac{u_3}{d}\right), \quad (33)$$

with  $\omega_1$  is the fundamental natural frequency. The constraints for clamped-clamped boundaries are:  $u = w = \theta = 0$  at  $x = 0, L$ .

##### 4.1. Verification

The derived beam element is firstly verified in this sub-section by comparing the obtained result in the present work with the published data. In Tables 1 and 2, the static and dynamic pull-in voltages obtained in this paper are compared with that of Refs. [10, 11, 22]. The static pull-in voltages in these tables are obtained for a microbeam with the following material and geometric data:  $E = 169 \text{ GPa}$ ,  $\nu = 0.06$ ,  $b = 50 \text{ }\mu\text{m}$ ,  $h = 3 \text{ }\mu\text{m}$ ,  $\eta = 0$ . Different values for the total beam length  $L$  ( $\mu\text{m}$ ), the air-gap  $d$  ( $\mu\text{m}$ ) and the  $P/A$  (MPa) are considered in the tables. It can be seen from the tables that for all the considered beam length, air gap, axial force and the damping coefficient the static and dynamic pull-in voltages obtained herein agree well with the results of the cited references. It is worthy to note that the results of Ref. [11] are also based on the finite element method, while that of Refs. [10, 22] are used the finite difference method and the 3D MEMCAD model, respectively. The difference in the result obtained herein with that

of the cited references is caused by the different beam theories and methods used in the studies. It is noted that the Euler–Bernoulli beam theory was adopted in Ref. [10].

Table 1. Comparison of static pull-in voltages for an air gap  $d = 1 \mu\text{m}$

Sources	$L = 250 \mu\text{m}$			$L = 350 \mu\text{m}$		
	$P/A = -25$	$P/A = 0$	$P/A = 100$	$P/A = -25$	$P/A = 0$	$P/A = 100$
Ref. [10]	33.04	39.13	58.84	13.27	20.36	36.99
Ref. [22]	33.70	39.50	56.90	13.80	20.30	35.40
Present	33.11	39.59	58.32	12.88	20.20	36.52

Table 2. Comparison of dynamic pull-in voltages

$d(\mu\text{m})$	Sources	$P/A = -25 \text{ MPa}$		$P/A = 0$		$P/A = 100 \text{ MPa}$	
		$c_0 = 0.325$	$c_0 = 1.3$	$c_0 = 0.4$	$c_0 = 1.6$	$c_0 = 0.55$	$c_0 = 2.2$
1	Ref. [11]	32.3	33.1	38.8	39.6	56.8	58.3
	Present	32.5	33.2	38.9	39.7	57.0	58.4
2	Ref. [11]	93.2	96.2	110.4	113.3	160.6	165.6
	Present	95.8	98.1	113.0	115.5	163.0	167.1

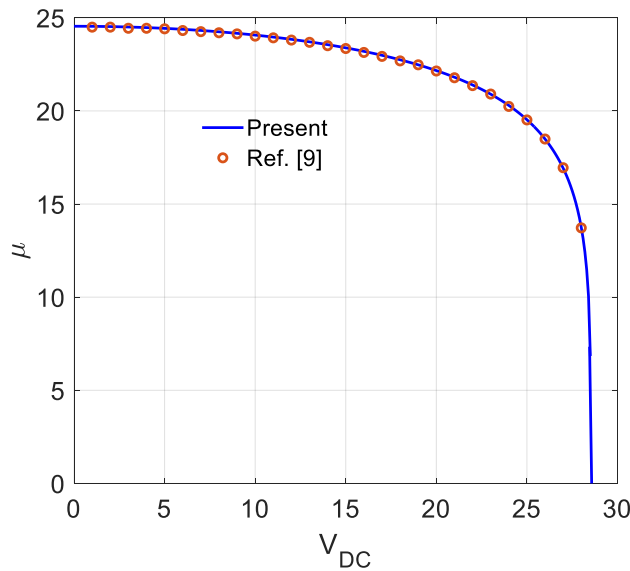


Fig. 2. Comparison of frequency parameter  $\mu$  versus applied voltage  $V_{DC}$  for  $h = 1.5 \mu\text{m}$  with an axial force  $P = -0.0009 \text{ N}$

The curve of frequency parameter  $\mu$  versus the applied voltage of the microbeam with an axial force  $P = -0.0009$  N is shown in Fig. 2 for a microbeam with  $L = 210$   $\mu\text{m}$ ,  $b = 100$   $\mu\text{m}$ ,  $d = 1.18$   $\mu\text{m}$ ,  $h = 1.5$   $\mu\text{m}$  and  $\eta = 0$ . For the sake of comparison, the result of Ref. [9] obtained by the Galerkin method is also depicted in the figure. The figure shows a good agreement between the finite element method base result of the present work with that of Ref. [9]. In addition, as seen from the figure, the frequency parameter steadily decreases with increasing the applied voltage and it becomes zero at the pull-in voltage.

#### 4.2. Numerical results

The effects of the material length scale and the axial force on the vibration of the clamped-clamped microbeam are investigated in this subsection. The static pull-in voltage is the minimum voltage at which the fundamental frequency of the microbeam becomes zero. In addition, the dynamic pull-in voltage is the smallest voltage that the gap between the two microbeam and the electrode will approach zero after a sufficiently large period of time.

The influence of the axial force on the frequency parameter and static pull-in voltage of the microbeam is illustrated in Fig. 3, where the applied voltage  $V_{DC}$  versus the fundamental frequency parameter  $\mu$  is depicted for  $\eta = 0$ ,  $L = 250$   $\mu\text{m}$ ,  $b = 50$   $\mu\text{m}$ ,  $\nu = 0.06$ ,  $E = 169/(1 - \nu^2)$  GPa,  $d = 1$   $\mu\text{m}$ ,  $h = 3$   $\mu\text{m}$ . As can be seen from the figure, both the frequency and the static pull-in voltage are decreased by increasing the compressive axial force, and they are increased by the tensile axial force. This result can be explained by the fact that the addition of a compressive axial force leads to a decrease of the beam flexural stiffness, while the tensile axial force results in an increase of the beam bending rigidity as in case of the macro beams [29].

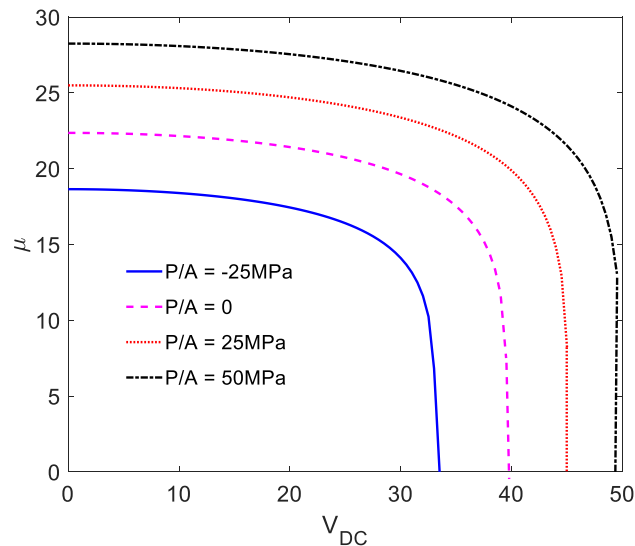


Fig. 3. Applied voltage versus frequency parameter for different axial forces ( $\eta = 0$ )

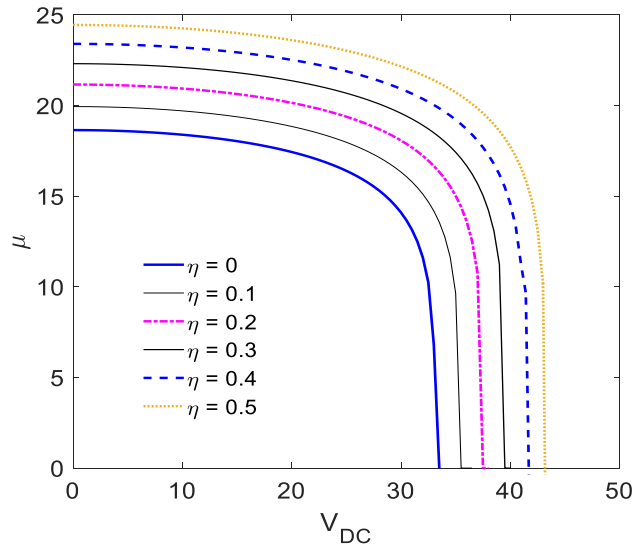


Fig. 4. Applied voltage versus frequency parameter for different  $\eta$  ( $P/A = -25$  MPa)

The effects of the length scale parameter on the frequency parameters and static pull-in voltages of the microbeam are illustrated in Fig. 4, where the applied voltage versus the fundamental frequency parameter of the microbeam is shown for various values of the material length scale parameter  $\eta$ . At a given value of the  $V_{DC}$  voltage, as can be seen from Fig. 4, the frequency parameter  $\mu$  and the static pull-in voltage increase by increasing the material length scale. The results in the figure reveal that the material length scale parameter has an important role on the fundamental frequency of the microbeam, and the frequency parameter is significantly underestimated when the microsize effect is ignored. Furthermore, the pull-in voltage corresponding to a zero fundamental frequency of the microbeam is also increased by the increase of the tensile axial force and the scale parameter  $\eta$ .

Finally, the curves for the relationship between the maximum deflection with the pull-in time are respectively illustrated in Figs. 5 and 6 for different values of the axial force and the material length scale parameter for the beam with  $L = 250 \mu\text{m}$ ,  $b = 50 \mu\text{m}$ ,  $h = 3 \mu\text{m}$ ,  $d = 1 \mu\text{m}$ ,  $E = 169 \text{ GPa}$ ,  $\nu = 0.06$ , and  $c_0 = 1.6 \text{ kg/s.m}$ . The stated data of the microbeam have been taken from Refs. [9,10,22], and the material length scale parameter  $\eta = 0$  is used for Fig. 5, and  $P/A = -25 \text{ MPa}$  is for Fig. 6. Fig. 5 shows that the time necessary for the deflection to attain the maximum value decreases by increase of tensile force. Similar to the effect of the axial force, the time at which the deflection attained the maximum value tends to be decreased by the increase of the material length scale parameter. It should be emphasized that the time value corresponding to  $W_{max} = 1$  is the pull-in time at which the gap between the microbeam and the electrode becomes zero. This time is generally decreased with the decrease of the dynamic pull-in voltage.

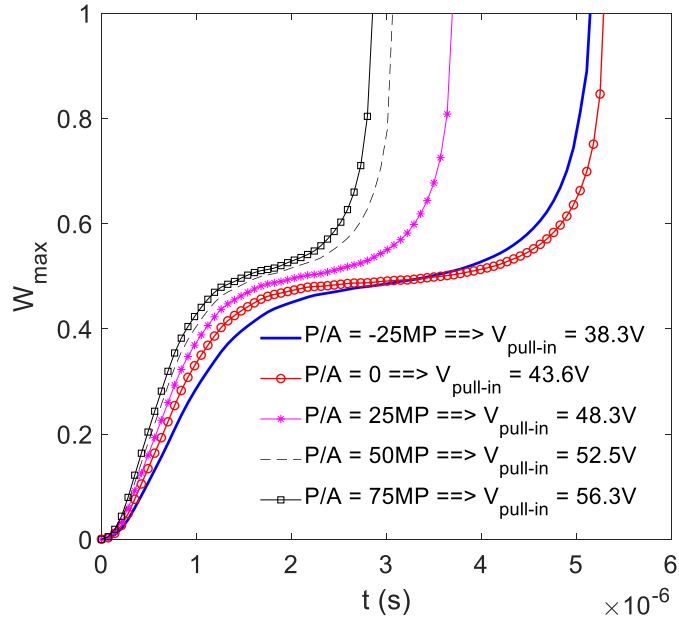


Fig. 5. Relation between maximum deflection with time for different values of axial force

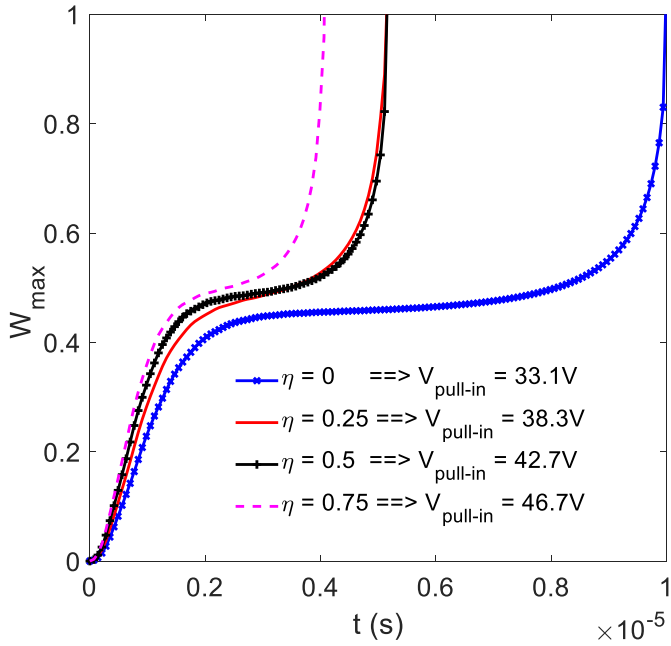


Fig. 6. Relation between  $W_{max}$  with time for different length scale parameters

## 5. CONCLUSIONS

The vibration of Timoshenko microbeams with an axial force under electric actuation in MEMS has been studied by using a nonlinear finite element procedure. Based on the modified couple stress theory and the von Kármán geometric nonlinearity, a two-node beam element was formulated and used to construct the discretized equation of motion. To avoid the shear-locking problem, the hierarchical functions have been employed to interpolate the displacement field. Using the derived beam element, the vibration characteristics, including the fundamental frequency and the maximum deflection, have been computed for the silicon microbeam with clamped-clamped ends by using the Newton-Raphson based iterative procedure in combination with the Newmark method. The influence of the applied voltage, the axial force as well as the microsize effect on the vibration behaviour of the microbeam has been studied in detail. It can be concluded from the numerical investigations that both the axial force and the microsize effect have a significant influence on the vibration frequencies and the pull-in voltages of the microbeam. The fundamental frequencies are underestimated by ignoring the microsize effect, while the beam deflections are overestimated when ignoring this effect.

## DECLARATION OF COMPETING INTEREST

The authors declare that they have no known competing financial interests or personal relationships that could have appeared to influence the work reported in this paper.

## FUNDING

This research received no specific grant from any funding agency in the public, commercial, or not-for-profit sectors.

## REFERENCES

- [1] J. Y. Park, G. H. Kim, K. W. Chung, and J. U. Bu. Monolithically integrated micromachined RF MEMS capacitive switches. *Sensors and Actuators A: Physical*, **89**, (2001), pp. 88–94. [https://doi.org/10.1016/S0924-4247\(00\)00549-5](https://doi.org/10.1016/S0924-4247(00)00549-5).
- [2] R. K. Gupta. *Electrostatic pull-in test structure design for in-situ mechanical property measurements of microelectromechanical systems (MEMS)*. PhD thesis, Massachusetts Institute of Technology, (1997).
- [3] B. Choi and E. G. Lovell. Improved analysis of microbeams under mechanical and electrostatic loads. *Journal of Micromechanics and Microengineering*, **7**, (1997), pp. 24–29. <https://doi.org/10.1088/0960-1317/7/1/005>.
- [4] E. M. Abdel-Rahman, M. I. Younis, and A. H. Nayfeh. Characterization of the mechanical behavior of an electrically actuated microbeam. *Journal of Micromechanics and Microengineering*, **12**, (2002), pp. 759–766. <https://doi.org/10.1088/0960-1317/12/6/306>.
- [5] M. I. Younis, E. M. Abdel-Rahman, and A. Nayfeh. A reduced-order model for electrically actuated microbeam-based MEMS. *Journal of Microelectromechanical Systems*, **12**, (2003), pp. 672–680. <https://doi.org/10.1109/jmems.2003.818069>.

- [6] M. I. Younis and A. H. Nayfeh. A study of the nonlinear response of a resonant microbeam to an electric actuation. *Nonlinear Dynamics*, **31**, (1), (2003), pp. 91–117. <https://doi.org/10.1023/a:1022103118330>.
- [7] E. M. Abdel-Rahman and A. H. Nayfeh. Secondary resonances of electrically actuated resonant microsensors. *Journal of Micromechanics and Microengineering*, **13**, (2003), pp. 491–501. <https://doi.org/10.1088/0960-1317/13/3/320>.
- [8] S. Chatterjee and G. Pohit. A large deflection model for the pull-in analysis of electrostatically actuated microcantilever beams. *Journal of Sound and Vibration*, **322**, (2009), pp. 969–986. <https://doi.org/10.1016/j.jsv.2008.11.046>.
- [9] M. I. Younis. *MEMS linear and nonlinear statics and dynamics*. Springer US, (2011). <https://doi.org/10.1007/978-1-4419-6020-7>.
- [10] G. Rezaadeh, H. Sadeghian, I. Hosseinzadeh, and A. Toloie. Investigation of pull-in phenomenon on extensible micro beam subjected to electrostatic pressure. *Sensors & Transducers Journal*, **79**, (5), (2007), pp. 1173–1179.
- [11] M. R. Ghazavi, G. Rezaadeh, and S. Azizi. Finite element analysis of static and dynamic pull-in instability of a fixed-fixed micro beam considering damping effects. *Sensors & Transducers*, **103**, (4), (2009), p. 132.
- [12] A. J. Kaneria, D. S. Sharma, and R. R. Trivedi. Static analysis of electrostatically actuated micro cantilever beam. *Procedia Engineering*, **51**, (2013), pp. 776–780. <https://doi.org/10.1016/j.proeng.2013.01.111>.
- [13] J.-H. Kuang and C.-J. Chen. The nonlinear electrostatic behavior for shaped electrode actuators. *International Journal of Mechanical Sciences*, **47**, (2005), pp. 1172–1190. <https://doi.org/10.1016/j.ijmecsci.2005.04.006>.
- [14] D. C. C. Lam, F. Yang, A. C. M. Chong, J. Wang, and P. Tong. Experiments and theory in strain gradient elasticity. *Journal of the Mechanics and Physics of Solids*, **51**, (2003), pp. 1477–1508. [https://doi.org/10.1016/s0022-5096\(03\)00053-x](https://doi.org/10.1016/s0022-5096(03)00053-x).
- [15] M. H. Kahrobaiyan, M. Asghari, M. Rahaeifard, and M. T. Ahmadian. A nonlinear strain gradient beam formulation. *International Journal of Engineering Science*, **49**, (2011), pp. 1256–1267. <https://doi.org/10.1016/j.ijengsci.2011.01.006>.
- [16] F. Yang, A. C. M. Chong, D. C. C. Lam, and P. Tong. Couple stress based strain gradient theory for elasticity. *International Journal of Solids and Structures*, **39**, (2002), pp. 2731–2743. [https://doi.org/10.1016/s0020-7683\(02\)00152-x](https://doi.org/10.1016/s0020-7683(02)00152-x).
- [17] H. Farokhi and M. H. Ghayesh. Size-dependent behaviour of electrically actuated microcantilever-based MEMS. *International Journal of Mechanics and Materials in Design*, **12**, (2015), pp. 301–315. <https://doi.org/10.1007/s10999-015-9295-0>.
- [18] M. H. Ghayesh and H. Farokhi. Nonlinear behaviour of electrically actuated microplate-based MEMS resonators. *Mechanical Systems and Signal Processing*, **109**, (2018), pp. 220–234. <https://doi.org/10.1016/j.ymsp.2017.11.043>.
- [19] M. Baghani. Analytical study on size-dependent static pull-in voltage of microcantilevers using the modified couple stress theory. *International Journal of Engineering Science*, **54**, (2012), pp. 99–105. <https://doi.org/10.1016/j.ijengsci.2012.01.001>.
- [20] M. H. Ghayesh, H. Farokhi, and M. Amabili. Nonlinear behaviour of electrically actuated MEMS resonators. *International Journal of Engineering Science*, **71**, (2013), pp. 137–155. <https://doi.org/10.1016/j.ijengsci.2013.05.006>.
- [21] Y. C. Hu, C. M. Chang, and S. C. Huang. Some design considerations on the electrostatically actuated microstructures. *Sensors and Actuators A: Physical*, **112**, (2004), pp. 155–161. <https://doi.org/10.1016/j.sna.2003.12.012>.

- [22] P. M. Osterberg and S. D. Senturia. M-TEST: A test chip for MEMS material property measurement using electrostatically actuated test structures. *Journal of Microelectromechanical Systems*, **6**, (1997), pp. 107–118. <https://doi.org/10.1109/84.585788>.
- [23] C. I. Le, Q. D. Tran, V. D. Lam, and D. K. Nguyen. Size-dependent behavior of a MEMS microbeam under electrostatic actuation. *Vietnam Journal of Mechanics*, **44**, (2022), pp. 69–81. <https://doi.org/10.15625/0866-7136/16834>.
- [24] R. P. Shimpi and H. G. Patel. Free vibrations of plate using two variable refined plate theory. *Journal of Sound and Vibration*, **296**, (2006), pp. 979–999. <https://doi.org/10.1016/j.jsv.2006.03.030>.
- [25] R. D. Cook. *Concepts and applications of finite element analysis*. John Wiley & Sons, (2007).
- [26] D. K. Nguyen and V. T. Bui. Dynamic analysis of functionally graded Timoshenko beams in thermal environment using a higher-order hierarchical beam element. *Mathematical Problems in Engineering*, **2017**, (2017), pp. 1–12. <https://doi.org/10.1155/2017/7025750>.
- [27] J. E. Akin. *Finite elements for analysis and design: computational mathematics and applications series*. Elsevier, (2014).
- [28] A. Tessler and S. B. Dong. On a hierarchy of conforming timoshenko beam elements. *Computers & Structures*, **14**, (1981), pp. 335–344. [https://doi.org/10.1016/0045-7949\(81\)90017-1](https://doi.org/10.1016/0045-7949(81)90017-1).
- [29] A. Ghali, A. M. Neville, and T. G. Brown. *Structural analysis: A unified classical and matrix approach*. CRC Press, 6th edition, (2017).